

We are IntechOpen, the world's leading publisher of Open Access books Built by scientists, for scientists

6,900

Open access books available

186,000

International authors and editors

200M

Downloads

Our authors are among the

154

Countries delivered to

TOP 1%

most cited scientists

12.2%

Contributors from top 500 universities



WEB OF SCIENCE™

Selection of our books indexed in the Book Citation Index
in Web of Science™ Core Collection (BKCI)

Interested in publishing with us?
Contact book.department@intechopen.com

Numbers displayed above are based on latest data collected.
For more information visit www.intechopen.com



Galactic Cosmic Rays from 1 MeV to 1 GeV as Measured by Voyager beyond the Heliopause

William R. Webber

Additional information is available at the end of the chapter

<http://dx.doi.org/10.5772/intechopen.75877>

Abstract

Voyager 1 has now been beyond the heliopause for over 5 years since its seminal crossing of this boundary in August of 2012. During its epic 40 year journey of ~122 AU out to this boundary and beyond this spacecraft has passed through several regions of the heliosphere including the heliosheath of extent ~30 AU just inside the heliopause (HP), where extremely large and variable intensities of protons, helium and oxygen nuclei as well as electrons between 1 and 100 MeV were observed. Then, suddenly these particles completely vanished and new and completely different spectra of particles between 1 MeV up to ~1 GeV and beyond, instantly recognizable as those for galactic cosmic rays were observed. These spectra and intensities at all energies have remained constant to within $\pm 1\%$ for 5 years corresponding to 20 AU beyond the HP.

Keywords: cosmic rays, dark matter, heliosphere, acceleration

1. Introduction

Voyager 1 has now been beyond the heliopause for over 5 years since its seminal crossing of this boundary in August of 2012. During its epic 40 year journey of ~122 AU out to this boundary and beyond this spacecraft has passed through several regions of the heliosphere including the heliosheath of extent ~30 AU just inside the heliopause (HP) where extremely large and variable intensities of protons, helium and oxygen nuclei as well as electrons between 1 and 100 MeV were observed. See earlier article in Astrophysics [1] showing and discussing these intensity time profiles.

Then, suddenly these particles completely vanished and new and completely different spectra of particles between 1 MeV up to ~ 1 GeV, instantly recognizable as those for galactic cosmic rays, were observed. These LIS intensities at all energies have remained constant to within $\pm 1\%$ for 5 years corresponding to 20 AU beyond the HP. These low energy galactic spectra and their relation to higher energy measurements such as those made by AMS-2 will be discussed in this paper in terms of the acceleration, source distribution and propagation of cosmic rays in the galaxy.

We begin in this paper by discussing the radial intensity profiles outward from the Earth through the heliosphere and beyond into interstellar space. We will compare these intensity profiles for electrons and protons, from the lowest energies, ~ 1 MeV, to the higher energies of a few hundred MeV which are normally considered as cosmic rays. The profiles provide a graphic view of the scale of the various regions of the heliosphere and the entrance into the uncharted regions of interstellar space and the realm of galactic cosmic rays.

We will then discuss the spectra of galactic cosmic ray electrons, protons, helium and heavier nuclei that are measured for the 1st time by Voyager. Every step in this process provides a new insight into the features of these galactic cosmic rays that could never be studied previously because of our location within the heliosphere.

2. The radial intensity vs. time profiles

Figure 1 shows radial intensity profiles for the two lowest energy electron channels, the HET A1-A2 stop channel at $\sim 0.7 \pm 0.3$ MeV and the HET B1-B2-C4 stop channel with a peak response

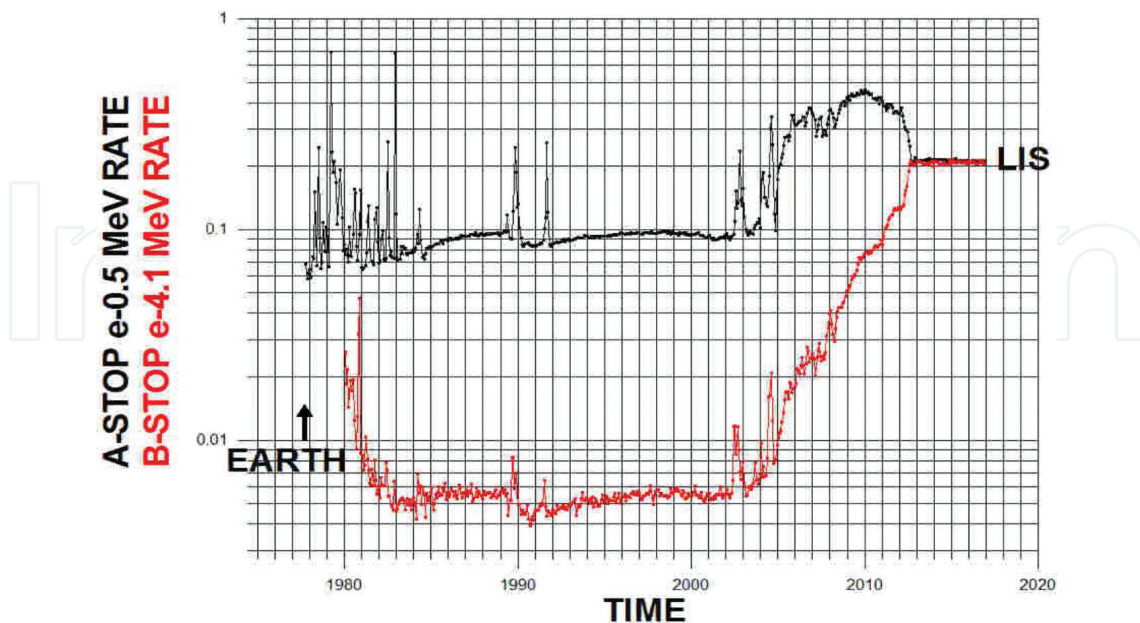


Figure 1. Time history of 26 day average intensities of A-stop 0.7 MeV (in black) and 4 MeV B stop electrons (in red) from launch at Earth 1977 to the end of data in 2017, at ~ 140 AU. These rates provide radial and temporal intensity profiles. The B-stop rate is normalized to A-stop rate of $0.21 \text{ c} \cdot \text{s}^{-1}$ in LIS using the factor 0.75.

between 3.0 and 4.0 MeV, from the time of launch (1977) to the present time (2018). These energy responses are determined by extensive GEANT-4 calculations. These telescopes are described in [2, 3]. The two intensities are normalized to those observed in local interstellar space (LIS).

One can define from **Figure 1** four temporal or spatial regions that apply to all the components and energies discussed here. The 1st region is from launch in 1977 to 1983.0 when V1 was at about 20 AU and also near its maximum latitude of $+30^\circ$. This region (nearest the Sun) is punctuated by many abrupt increases related to interplanetary propagating electron events of energy <1 MeV of solar origin. These are closely coordinated with observations inside the Earth's orbit from HELIOS during the 1977–1978 time period. The individual events are separated temporally at Voyager and HELIOS. Also included is the Jupiter encounter occurring at ~ 1979.2 .

The second region (time period) is from 1983.0 to 2005.0 at which time V1 crossed the HTS and entered the heliosheath at ~ 95.0 AU and at $+30^\circ$. The effects of the solar 11 year modulation cycle are rather weakly seen in this region. These variations are similar temporally to what was observed for higher energy protons [4] and shown later in **Figure 3**. Two massive solar induced interplanetary electron events are seen in the A stop rate in 1989 and 1991 when V1 was at between 40 and 50 AU. These events are related to large shocks moving outward in the heliosphere with speeds close to 1000 km/s.

During the time V1 is in the heliosheath region from 2005.0 to 2012.65 between 95 and 121.7 AU (Region 3) there is a factor of 3–4 increase in the sub-MeV electron intensities which, during most of this time period, have even higher intensities than those observed beyond the HP, in the local interstellar medium. These are electrons accelerated in the heliosheath. Meanwhile the intensity of the 4 MeV electrons increases in the heliosheath from the HTS crossing to the HP by a factor ~ 30 . This is believed to be a result of modulation effects in the heliosheath which reduce the LIS intensity of these higher energy electrons.

Beyond the heliopause (HP) in LIS the electron intensities have remained constant to within $\pm 1\%$ at both energies for 5 years (~ 18 AU of outward travel for V1). Notice that the intensities of these electrons in LIS are higher than those at the Earth by a factor ~ 4 at 0.7 MeV and by a factor ~ 20 at 4 MeV. These differences are due in part to solar modulation effects and in part to the local acceleration of 0.7 MeV electrons.

In **Figure 2** we show the 1.8–2.6 MeV proton intensity, again normalized to the LIS value that is measured for 0.7 MeV electrons. This is the lowest energy part of the interstellar proton spectrum that can be measured on Voyager in a 2-D, dE/dx, telescope mode. It represents a limit to the characteristics of the lower energy proton propagation in the galaxy from the nearest sources in the galaxy since it corresponds to only $\sim 35\mu$ of equivalent Si traversed during the galactic propagation.

In region 1, between launch and 1983 and inside ~ 20 AU, the Earth and the inner heliosphere are bathed in an almost continuous flux of 2 MeV protons which exceeds the possible background galactic cosmic rays at this energy and location by a factor ~ 1000 and is comparable to the intensities observed further out in the heliosheath. This continuously high intensity results from the 1.8 to 2.6 MeV protons from many individual solar events, with the intensities piling up due to the large longitudinal diffusion.

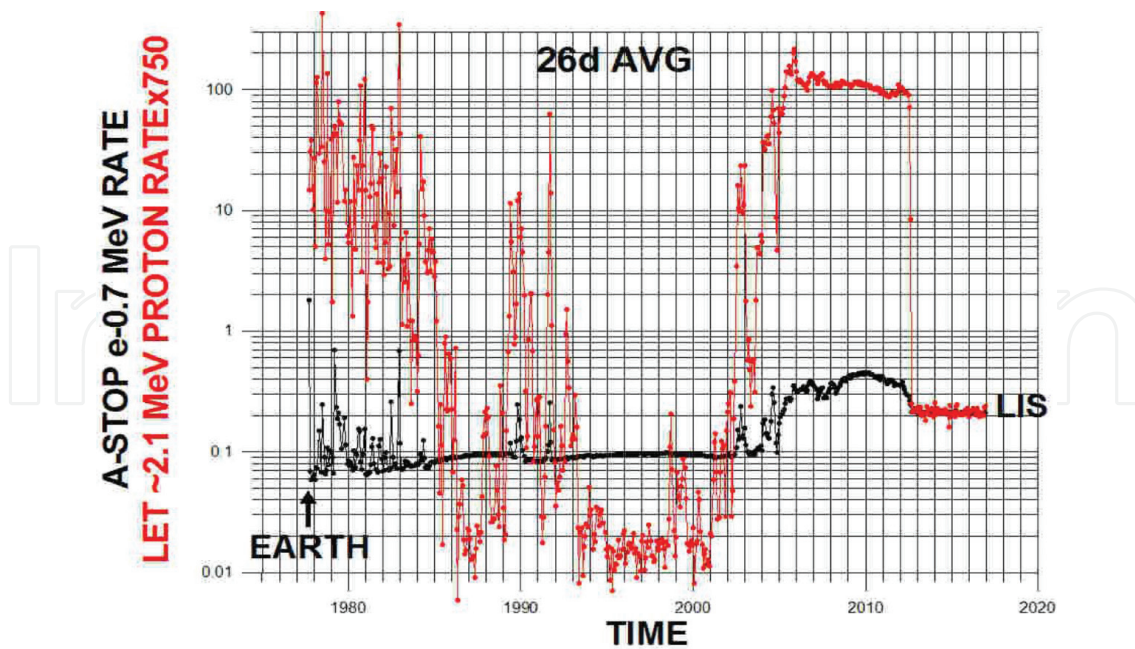


Figure 2. Same as **Figure 1**. The L1-L2 stop 1.8–2.6 MeV proton rate (in red) is normalized to the A-stop 0.7 MeV LIS electron rate using the factor $\times 750$.

In region 2, between ~ 20 AU and the HTS at 95 AU, these 2 MeV proton intensities reach a level which is less than that in LIS. This corresponds to a solar activity minimum and also to solar modulation minimum. This intensity, which is up to a factor ~ 12 times less than the LIS intensity, could be a representation of the level of solar modulation of these particles at this low energy of ~ 2 MeV.

In region 3, the intensity of these low energy protons increases by a factor 1000 beyond the HTS. It remains at this high level for a distance ~ 30 AU as a result of heliosheath accelerated protons. Then suddenly the intensity decreases by a factor ~ 500 corresponding to a distance of ~ 0.1 AU near the HP. This intensity change over such a small radial interval requires a remarkably effective particle barrier at the HP.

In region 4, beyond the HP, the proton intensity represents the low energy tail of the galactic proton spectrum with an intensity ~ 0.5 of that at the intensity peak of the differential spectrum which occurs at ~ 30 MeV.

In **Figure 3** we show the higher energy proton (250 MeV) intensity time profile from the solar modulation study in [4]. This proton intensity is also normalized to the 0.7 MeV A1-A2 stop LIS electron intensity beyond the HP. The solar modulation effects are seen in region 1 inside 20 AU where the Voyager observations for 250 MeV protons blend in well with spacecraft observations of this modulation near the Earth and also neutron monitor observations [5–7] at the same time. The intensity at the Earth at this energy is a factor ~ 8 below the LIS values.

In region 2, between about 20 and 95 AU, solar 11 year modulation effects are observed at 250 MeV which are in synch in both time and magnitude with those observed at the Earth, but with a time delay corresponding to outward moving structural features with a speed $\sim 600 \text{ km}\cdot\text{s}^{-1}$.

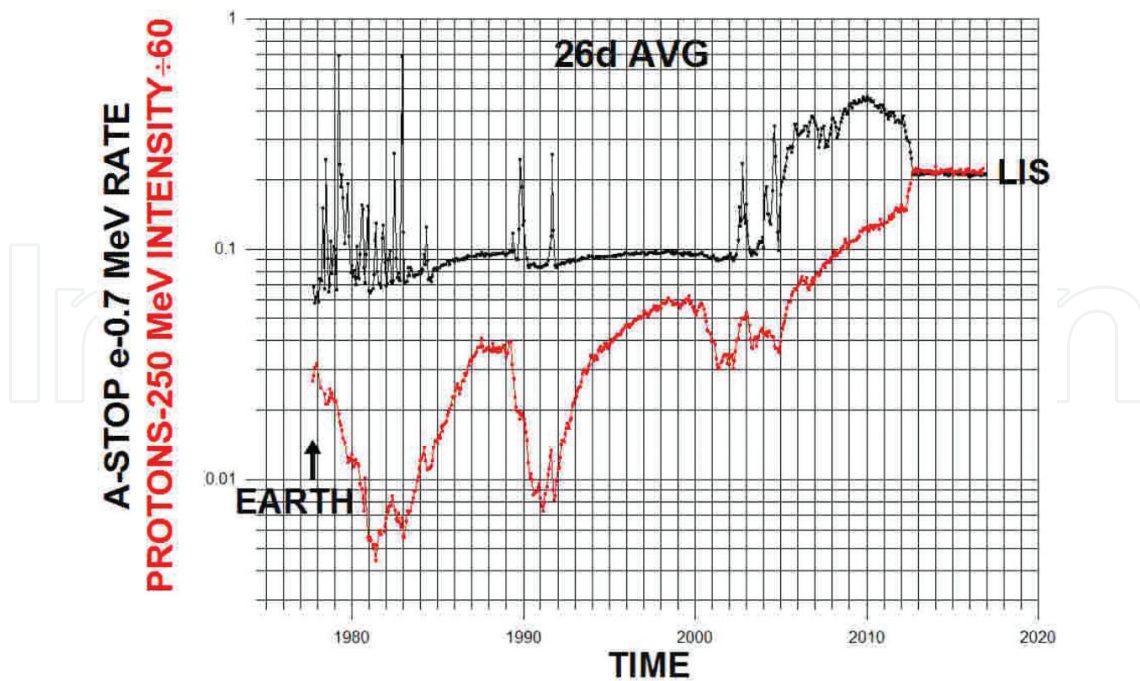


Figure 3. Same as **Figure 1**. The 250 MeV proton intensity in $\text{p}/\text{m}^2\text{-sr}\cdot\text{s}\cdot\text{MeV}$ (in red) is normalized to A-stop 0.7 MeV LIS electron rate using the factor $\div 60$.

Moving outward into region 3, we find that the intensity of these 250 MeV protons increases by a factor ~ 4 in the heliosheath. The large modulation beyond the HTS at this higher energy was previously unrecognized and amounts to $\sim 1/3$ of the total solar modulation of these particles in the heliosphere.

This solar modulation of these higher energy protons can be well described with a single modulation parameter ϕ corresponding to an energy loss resulting from a potential difference, ϕ in MV, between the observation point and the LIS spectrum [8]. This simple description arises from the fact that the overall spherically symmetric solar modulation in the heliosphere appears to follow the description provided by Louville's Theorem relating to the constancy for the particle density and momentum in phase space. Of course there are deviations from this simple picture due to structural features in the heliosphere such as the heliospheric current sheet, and also for the solar polarity changes which induce a 22 year cycle in the solar modulation process, but these other processes do not appear to dominate at these energies and above, where, in fact, the same value of ϕ derived from these protons also gives a good description of the historical neutron monitor observations of cosmic ray modulation effects at the Earth that have been carried out over the last 70 years.

Here we summarize the most general features of all of the radial intensity profiles. The most prominent feature is the sharpness and effectiveness of the heliospheric boundary, the heliopause. For low energy protons the reduction of intensity is a factor ~ 500 , taking place in only 1–26 day interval corresponding to less than 0.1 AU in distance.

The effects of this boundary on electrons are even more astounding. A radial intensity gradient $\sim 130\%/AU$ just inside the HP for 4 MeV electrons changes to a $0.1\%/AU$ radial gradient in

the LIM in just 1–26 day interval of ~ 0.1 AU in radius. Essentially whatever intensities exist in the heliosphere apparently stay in the heliosphere as a result of an almost impenetrable heliopause at these lower energies. As far as energetic particles go, the interstellar medium at this location has little recognition of the nearby heliosphere.

Other features of the heliosphere newly recognized from this study include: (1) The heliosheath is a very interesting and important region both in terms of accelerating protons and also (more weakly) electrons as well as for large solar modulation effects. The solar modulation effects on the intensity in this region range from a factor ~ 4 for ~ 1 GV protons to a factor ~ 100 for 15 MV electrons and then decrease to a factor ~ 30 for 4 MV electrons and much less for 1 MeV electrons which appear to be mostly locally produced.

The massive acceleration of nuclei, e.g., protons and He and O nuclei in the heliosheath, extending down to ~ 1 MeV and up to ~ 100 MeV/nuc, which was previously known and believed to be fueled by high ionization potential IS ions, is joined by the newly found acceleration of sub-MeV electrons.

The 11 year and longer solar activity cycles studied now for over 70 years using neutron monitors, balloon and spacecraft borne instruments at higher energies, and so important for geophysical studies [9], are still significant beyond the HTS. Even for protons at 250 MeV the intensity increase in the heliosheath region is a factor ~ 4 ; for electrons, this increase due to solar modulation reaches a maximum of a factor ~ 100 at ~ 15 MeV. These effects were previously unrecognized.

And finally the new observations reported here have also extended the V1 measurements of the local interstellar electron spectrum by a factor ~ 10 lower in energy (e.g., down to 0.5 MeV) as compared with even the initial Voyager measurements of [2] beyond the HP. For protons the minimum energy measured is now ~ 1.8 MeV, a factor ~ 2 times lower than the initial measurement for these particles. The intensities obtained at these lowest energies appear to be consistent with a smooth extension of those measured at higher energies as would be expected from propagation calculations. The range of the lowest energy electrons and protons is only $\sim 50 \mu$ of Si. This places severe constraints on the distribution of nearby sources of these particles but illustrates that, even at these lower energies, the spectra are still a compendium of many sources with an individuality obscured by diffusion in the galactic magnetic fields.

3. The galactic electron spectrum

Voyager has now measured the true LIS electron spectrum from ~ 1 to 60 MeV. When compared with simultaneous measurements of electrons by the PAMELA spacecraft near the Earth they indicate a solar modulation factor ~ 500 between the LIS spectrum and that measured at the Earth between about 10–100 MeV (**Figure 4**). At higher energies this modulation decreases. It is believed to be only a factor ~ 3 –4 at 1 GeV, decreasing to perhaps 20% at 10–20 GeV where high precision electron measurements are available from both PAMELA and AMS-2 [10, 11].

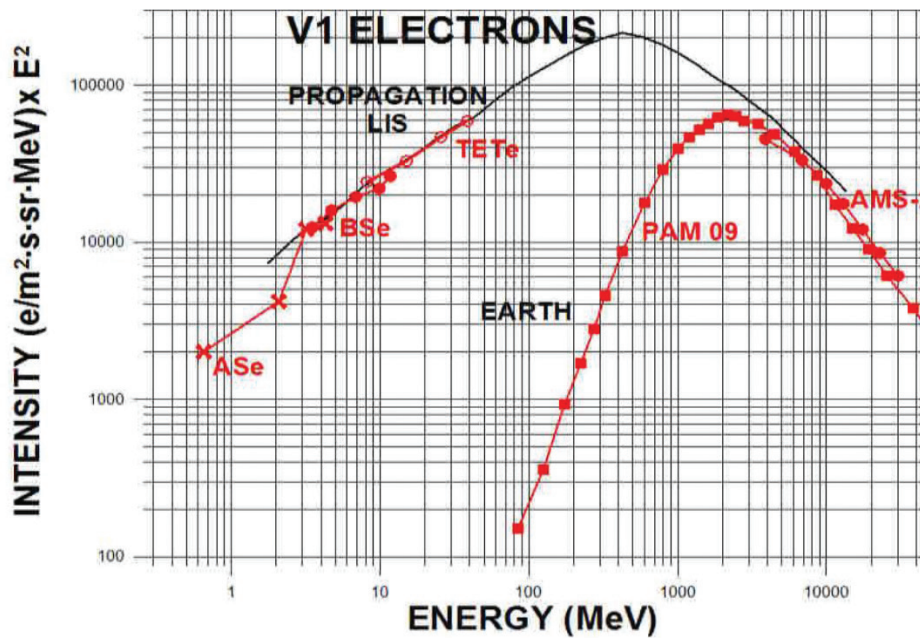


Figure 4. The electron spectrum measured at Voyager using the TET, B stop and A stop telescopes and the measurements of PAMELA and AMS-2 at higher energies. The figure is in a $\times E^2$ format. Note the severe solar modulation of electrons which amounts to a factor ~ 500 below 100 MeV and is still $\sim 20\%$ between 10–20 GeV/nuc. Also note the V1 spectrum which is $\sim E^{-1.3}$ between about 1–60 MeV. The black curve shows a Monte Carlo calculation with an electron source spectrum $\sim E^{-2.25}$ and a path length $\sim 20.6 \beta P^{-0.45}$ above 0.562 GV and with a diffusion coefficient $\sim P^{-1.0}$ below 0.562 GV.

Figure 4 shows the electron spectrum measured at Voyager and also in the higher energies where solar modulation effects are small. The plot is a $\times E^2$ presentation which shows both low and high energy differences. There is a large gap in the intermediate energy range for LIS electrons from ~ 100 MeV to several GeV. At energies above a few GeV the electron spectrum measured by PAMELA and AMS-2 steepens rapidly. Part of this increase in spectral index is due to synchrotron and inverse Compton energy loss which are $\sim E^2$. This high energy region is shown in **Figure 5** in a $\times E^3$ format. The AMS-2 data on electrons [11] is shown along with Monte Carlo propagation calculations of the electron spectrum using various source spectral indices [12, 13].

We have shown from these calculations that, in order to fit both low energy and high energy data, the source spectral exponent for electrons changes from being $\sim P^{-2.24}$ below about 8 GV to one $\sim P^{-2.4}$ at higher energies extending up to ~ 1 TV [12, 13].

At ~ 400 MeV, which is ~ 1.0 GV for protons there are corresponding measurements of the proton and electron intensities at the Earth by PAMELA and also at Voyager. The ratio of Voyager to PAMELA proton intensities at the two locations is ~ 4.0 which is caused by the amount of solar modulation between the LIS and the Earth at 1 GV. The electron intensity is also measured at this time by PAMELA and at 1 GV it is $2.5 \times 10^{-2} \times$ the proton intensity. We believe from solar modulation theory [8] that at 1 GV the total modulation of electrons and protons should be nearly the same. So the LIS electron intensity at 1 GV could be estimated from this approach to be $1.4\text{--}1.6 \times 10^{-1} \text{e/m}^2 \cdot \text{s} \cdot \text{sr} / \text{MeV}$. This intensity is very close to the value

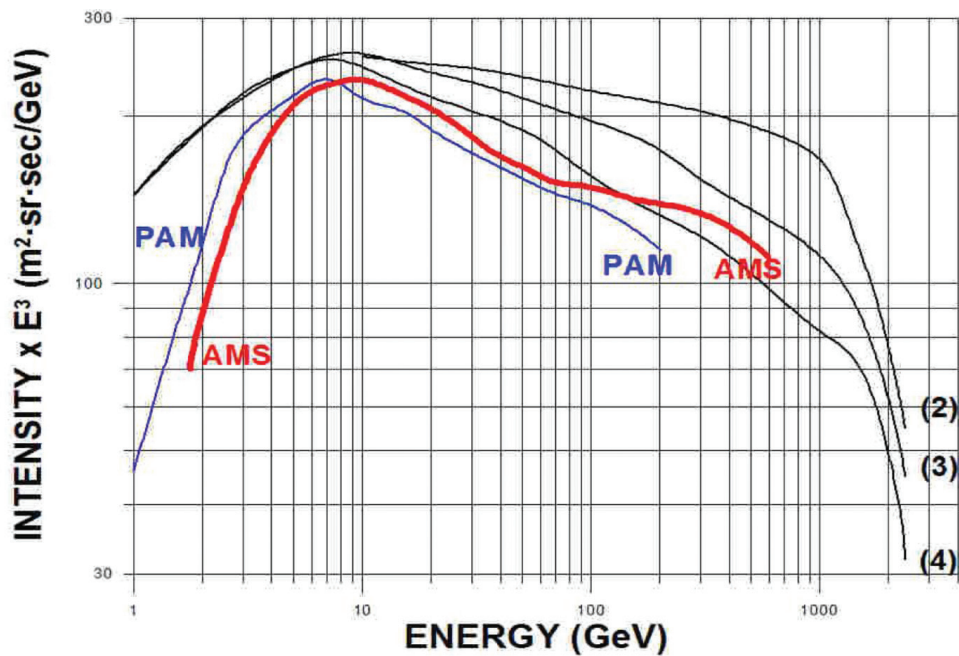


Figure 5. The electron spectrum above 1 GeV measured by AMS-2 [11] and PAMELA [10]. The black solid curves are for (1) a source electron spectrum $\sim E^{-2.25}$ at all energies and (2, 3 and 4) for electron source spectra $\sim E^{-2.25}$ below ~ 6 GeV and $P^{-2.30}$, $P^{-2.35}$ and $P^{-2.40}$ respectively above 6 GeV.

at 1 GV obtained in the Monte Carlo diffusion propagation models that fit the LIS at the low Voyager energies and the high energies measured by PAMELA or AMS-2 [12, 13].

In **Figure 6** we show the $e/H(E)$ interstellar ratios of intensities measured at both Voyager and at AMS-2 from a few MeV to 1 TeV. These ratios, in intensity/MeV, range from $\sim 10^2$ at 2 MeV to $\sim 3 \times 10^{-3}$ at 1 TeV, a difference of 3×10^5 and include the ratio between electron and proton intensities of 3.0×10^{-2} at 1 GV estimated above. This difference in low energy and high energy $e/H(E)$ ratios is mainly caused by propagation effects.

At lower rigidities this source ratio as a function of energy increases for a number of reasons. First of all there is the conversion between a differential energy and rigidity which depends on the different β of the particles. Then there is the dependence of the diffusion coefficient on $P^{-1.0}$ below 0.5 GV which affects only the electrons and decreases the $P^{-2.25}$ source index to $\sim P^{-1.3}$. And also there is the energy loss by ionization which eventually reduces the source spectral index for protons from a negative one to a positive value. At the higher energies the synchrotron and inverse Compton losses increase the source spectral index of electrons by almost 1.0 power thus reducing the e/H ratio.

Recall that we have assumed for electrons, that to fit the data at both low and high energies up to 1 TeV, source spectra of the form $dj/dE \sim P^{-2.24}$, below $\sim 6-8$ GV are needed with the exponent becoming ~ 2.40 at high rigidities [12, 13]. Very similar rigidity spectra with almost the same exponents and a break at $\sim 6-8$ GeV are required to simultaneously fit the Voyager low energy proton data and the high energy AMS-2 proton data, again from ~ 2 MeV to 1 TeV [15] (see following sections).

So in view of the above similarity of rigidity spectra for electrons and protons, the e/H ratio itself as a function of rigidity should be almost constant. This almost constant value of the e/H ratio occurs between 0.5 and 1.0 GV where loss processes for electrons and protons in the galaxy are about equal. This value of the ratio is about $3-10 \times 10^{-2}$ as shown in **Figure 6**.

This source ratio of e/H for galactic cosmic rays as a function of rigidity which has previously been hidden from measurements at the Earth and is related to the acceleration of the galactic cosmic rays, now provides a crucial measurement along with the possible spectral break at ~ 8 GV. If there are no other selection effects, this ratio could indicate the degree of ionization in the acceleration region.

And last but certainly not least, still regarding electrons, we should point out that the electron spectrum $\sim E^{-1.3}$ at low energies, just about 1.0 power less than the assumed source spectrum with exponent = -2.25 , may have profound significance. Unless the source spectrum has a 2nd break at ~ 0.3 GV, which seems unlikely, this flattening of the spectrum is caused by a break in the diffusion coefficient which becomes $\sim P^{-1.0}$ below ~ 0.5 GV. This break has been predicted [14]. As a result the diffusion coefficient becomes large and these lower energy electrons rapidly flow out of the extended disk of the galaxy [12, 13]. This fraction that escape the disk, calculated in a Monte Carlo diffusion model, becomes $\sim 90\%$ below ~ 100 MeV and is shown as a function of energy in **Figure 7** of [12]. These electrons, with a spectrum $\sim E^{-2}$ above ~ 1 MeV, flow outward through the halo and into the local intergalactic medium at essentially the speed of light. They populate the region with a negative charge. Because of their relatively low energy they are undetectable by radio emissions and could be considered a form of non-baryonic dark matter and energy. Perhaps more sobering is the thought that this process of charge

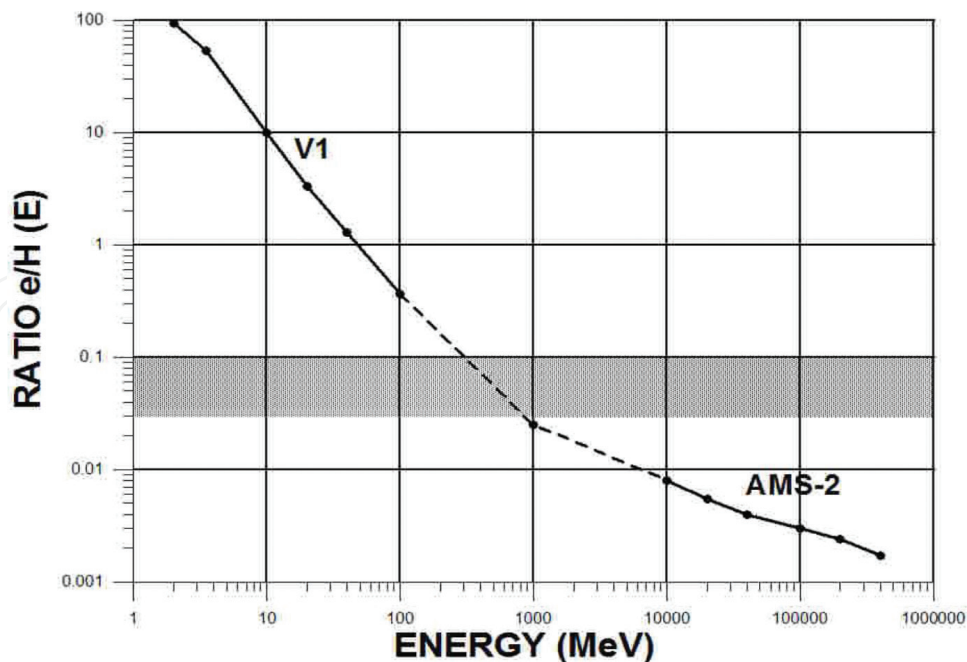


Figure 6. Ratios of intensity of electrons to protons as a function of energy, $e/H(E)$, measured by voyager and AMS-2 [10, 15] from 2 MeV to ~ 1 TeV. The estimated LIS value of the ratio at ~ 1 GeV as described below in the text is also shown.

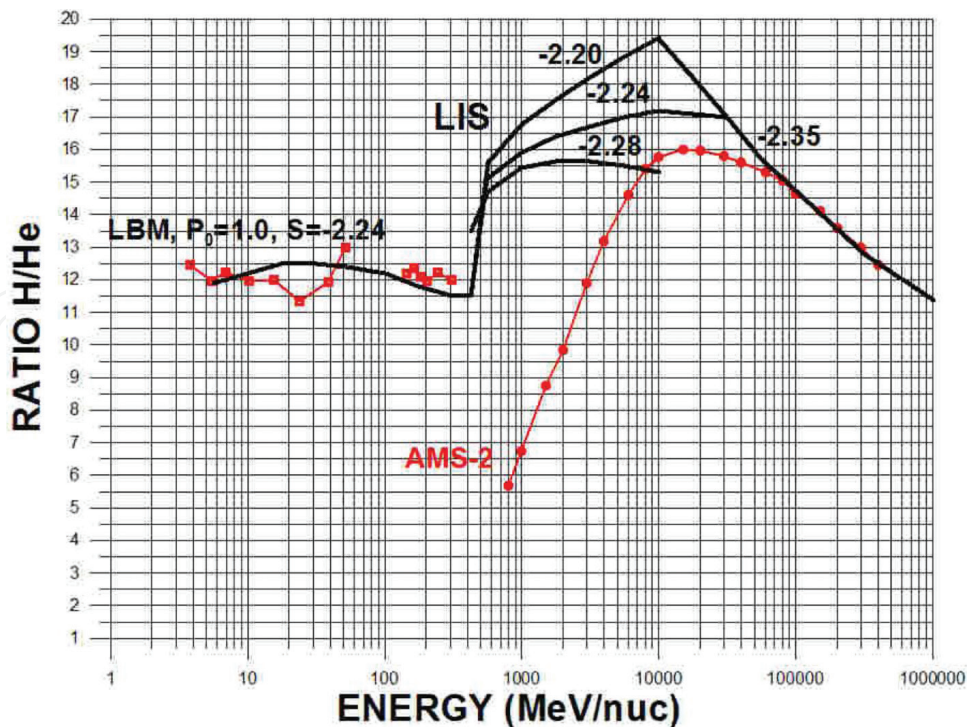


Figure 7. Ratios of hydrogen to helium nuclei intensities as a function of E/nuc as measured by Voyager between 10 and 350 MeV/nuc and by AMS2 [10, 15] above 1 GeV/nuc.

separation of leptons and protons could be going on throughout cosmic time, even stronger at earlier times, and as a result influence our interpretation of the expansion of the Universe.

4. The galactic hydrogen, helium and heavier nuclei spectra

As is the case for electrons, the interpretation of the Voyager measured LIS intensities of hydrogen, helium and heavier nuclei at low energies, and with no solar modulation, may be compared with the higher energy measurements from PAMELA or AMS-2 where the modulation becomes small. This provides a fulcrum of $\sim 10^5$ in energy to examine the spectra of the various nuclei. This is best done by examining the intensity ratios such as H/He, He/C, etc., along with the intensities themselves. Most of the measurements are in E/nuc , whereas the source spectra appear to be rigidity spectra so there is always a factor of at least β in converting from one representation to the other.

We begin this section by examining the spectra of H and He nuclei. **Figure 7** shows the ratio of intensities of H and He nuclei measured at Voyager at energies less than a few hundred MeV/nuc [3] and those at AMS-2 [15, 16] at energies from ~ 1 GeV/nuc up to 1 TeV/nuc. The Voyager measurements are consistent with a constant ratio ~ 12.5 , for H/He from ~ 10 MeV/nuc to ~ 350 MeV/nuc. This might suggest very similar H and He spectra in this energy range. The AMS-2 measurements obtain an E/nuc ratio ~ 16 at ~ 10 GeV/nuc, decreasing at both high and low energies. The decrease in this ratio at high energies where solar modulation effects are small, indicates different spectra for H and He nuclei, with a spectral index difference of

between -0.10 and -0.12 for either E/nuc or P spectra since at these high energies $\beta \rightarrow 1.0$. At lower energies the AMS-2 H/He (E) ratio decreases and reaches a value ~ 8 at 1 GeV/nuc. This is due to solar modulation effects. So the main goal of this study is to match the nearly constant LIS H/He (E) ratio of 12.5 measured by Voyager below ~ 300 MeV/nuc to the ratio of 16 measured at $\sim 10\text{--}20$ GeV/nuc by AMS-2.

These differences in ratios per E/nuc between a few hundred MeV/nuc and a few GeV/nuc immediately suggest a β dependence is involved and therefore when comparing ratios, source spectra as a function of rigidity is the appropriate parameter. We have found this to be the case in most comparisons of spectra of nuclei, particularly with different A/Z. So we now consider how the differences described above could be understood more simply in terms of source rigidity spectra. We assume that the source spectra of H and He nuclei are the same at rigidities below ~ 10 GV and can be represented by the formula.

$$dj/dP \sim P^{-S} \tag{1}$$

where we let S vary from -2.20 to -2.28 noting that we have already found that lower rigidity electrons are well described with a spectral index ~ -2.25 below ~ 10 GV.

The three solid black curves on **Figure 7** show the calculated H/He ratios after propagation in a LBM using source rigidity spectra for protons with $S = -2.20, -2.24$ and -2.28 all normalized to the Voyager measured value of 12.5 at 100 MeV/nuc. For the calculated curves above ~ 10 GV, we use a normalization to the AMS-2 measured ratios and with a source spectra index $= -2.36$ for

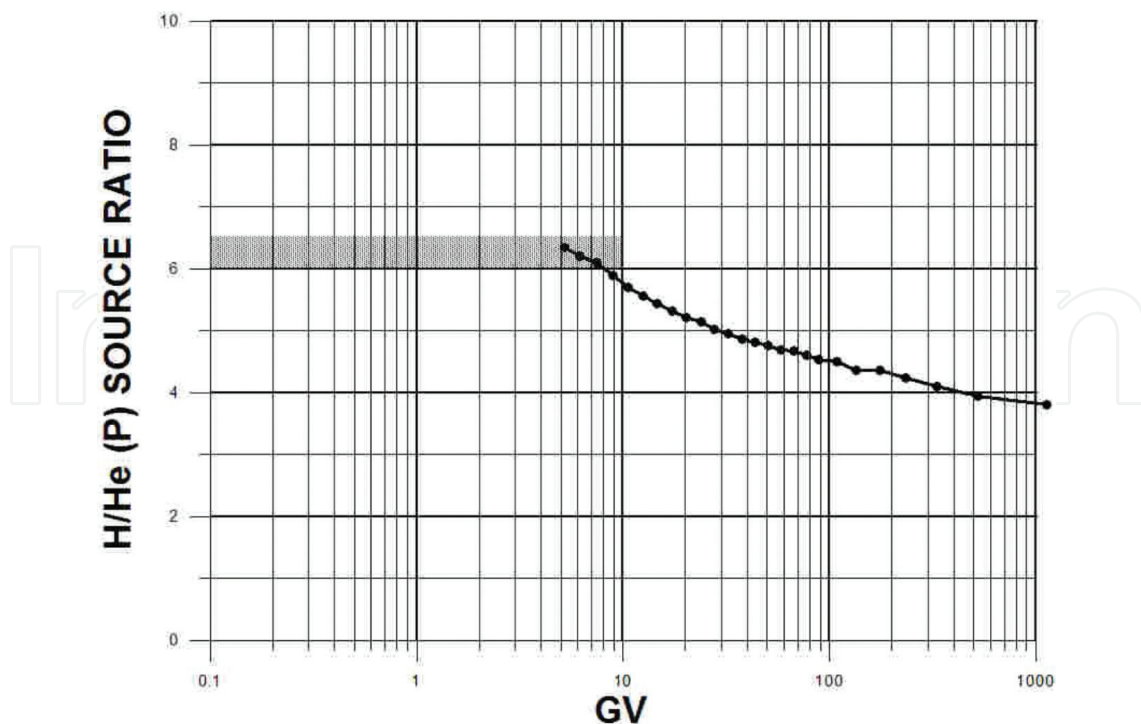


Figure 8. The LIS H/He (P) ratio as a function of rigidity. The data above ~ 8 GV where the solar modulation of this ratio is small is from AMS-2 [16].

protons, keeping the source spectral index at -2.24 for He nuclei. When a solar modulation of 10–20% in the H/He ratio at about 10 GV is included, a spectral index of -2.24 for both H and He nuclei gives the best fit at low energies along with that for a proton index of -2.36 at high energies and with a spectral break between 6 and 12 GV for protons.

The resulting H/He source ratio as a function of rigidity is very interesting. For this ratio we use the directly measured AMS-2 H/He (P) ratio above ~ 8 GV [16] as is shown in **Figure 8**. This ratio is ~ 3.5 at the highest rigidities increasing to ~ 6.0 at 8 GV. At lower rigidities the source ratio must become a constant because both H and He nuclei have identical rigidity spectra. This constant value depends on the exact details of the break, but we estimate the constant ratio of intensities at low rigidities to be between 6.0 and 6.5.

This ratio has important implications for the relative H and He abundances in the region where the main cosmic ray acceleration occurs. In terms of nucleons the ratio of 6.5 gives 63% protons and 37% Helium nucleons. The cosmological value in the case of big bang nucleosynthesis is usually taken to be $\sim 76\%$ protons and 24% Helium nucleons. Certainly interesting.

We now turn our attention to the comparison of the He and C spectra, again using a comparison of Voyager data on this ratio [3], which in this case extends up 1.5 GeV/nuc [4] and the AMS-2 data above 10 GeV/nuc [16, 17] where the solar modulation is small. The observed He/C (E) ratio from a few MeV/nuc to ~ 1 TeV/nuc is shown in **Figure 9**. It is seen to vary from

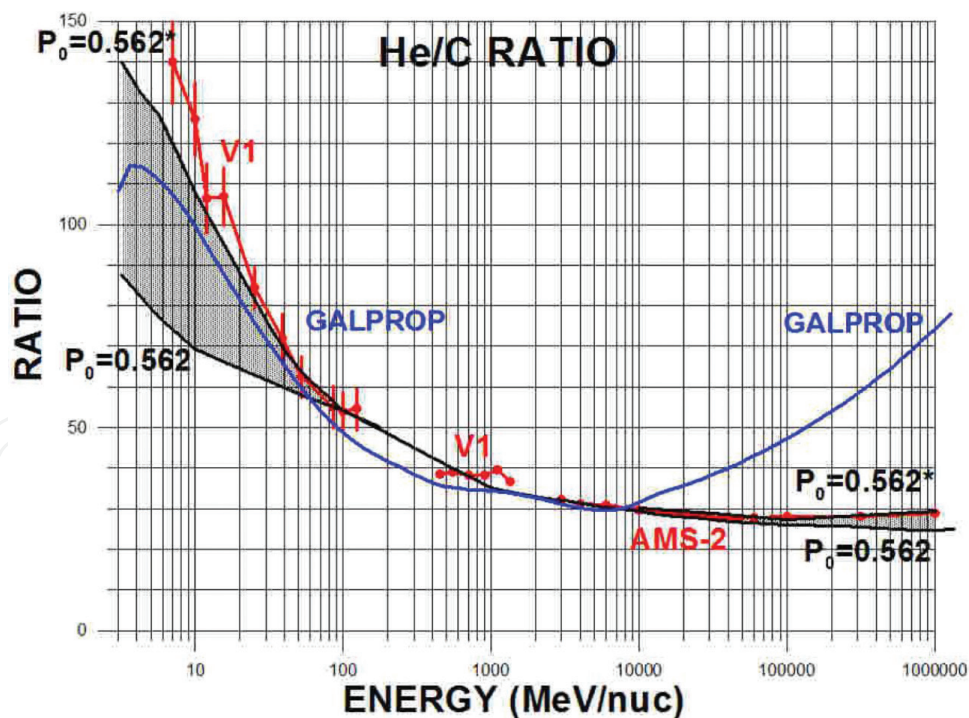


Figure 9. Observations and measurements of the He/C ratio between 3 MeV/nuc and 10^3 GeV/nuc. Errors on individual GeV/nuc voyager measurements are $\pm 5\%$. Errors on AMS-2 measurements are less than $\pm 2\%$. Black curve, labeled $P_0 = 0.562^*$, is for a truncated exponential PLD with mean path length $= \lambda = 20.6 \beta P^{-0.45}$ Above $P_0 = 0.562$ and with truncation parameters = 0.04 for He and 0.12 for C. The curve labeled $P_0 = 0.562$ is for a simple LBM with a PLD = exponential at all path lengths for $P_0 = 0.562$ GV. Dashed blue line is GALPROP calculation of the He/C ratio from [3].

~130 at low energies to about 27 at the highest energies. One might think that this observed ratio would be more or less constant if these nuclei had the same spectra, since they have the same A/Z ratio, etc., but it turns out that, when the actual intensities and spectral shapes are obtained from LBM propagation calculations [10], the observed He/C (E) ratios are reproduced with He and C rigidity spectra with a source spectral index ~ -2.24 for both components, extending throughout the rigidity range from ~ 100 MV to ~ 1.0 TV and with a source abundance He/C ratio = 23.7.

The reason for this is much like the case for electrons and protons, described earlier; it is mostly in the details of the LBM propagation, again in an overall simple LBM but with certain modifications at small matter path lengths, due possibly to the local distribution of the cosmic ray sources themselves. This modification (truncation) is perhaps the only significant departure from the incredible symmetry imposed by the LBM that is yet discerned from the Voyager studies to date. The details of the He/C ratio study are found in [18].

5. Spectral shapes of different nuclei at low energies

It has been possible to extend the earlier Voyager intensity and spectral measurements which were generally in the range 10–200 MeV/nuc [3] up to the GeV/nuc range and above [4]. This technique uses the precision measurement of ionization loss for particles that penetrate the 3 element total energy counters. The spectra of He, C, O, Mg, Si and Fe are obtained in this way up to 1.5 GeV/nuc, with an integral intensity at higher energies [4].

Spectra for these nuclei, including the lower energy Voyager measurements [3], are shown in **Figure 10**. The intensities are all normalized at 1.5 GeV/nuc. There is a dramatic charge dependence of the spectral shape that becomes more obvious at the lower energies. It is believed that these different charges have very similar and possibly identical source rigidity spectra. This identity of source spectra has been determined in the above section for He and C nuclei. In spite of the large dependence of the He and C ratio on energy which, changes from a value ~ 130 at 10 MeV/nuc to 27 at 1 TeV/nuc where AMS-2 measurements are available, the source spectra of both He and C nuclei are found to be $\sim P^{-2.24}$.

Most of the changes in the measured intensity ratios in **Figure 10** are due to the effects of propagation in the galaxy. The curves in **Figure 10** show these effects vividly. There is a Z dependent effect which becomes more prominent at the lower energies. Two sources of these effects are, (1) ionization energy loss in interstellar matter which is Z^2/β^2 , and (2) fragmentation collisions which are proportional to a $A^{1/3}$ dependence of these cross sections.

The ionization energy loss is particularly important at the lower energies because of the $1/\beta^2$ dependence, but even these ionization loss effects cannot account fully for the Z dependent turnovers of the differential spectra at lower energies. These differential spectra are observed to have maxima which systematically increase from ~ 30 MeV/nuc for He to ~ 100 MeV/nuc for Fe. The explanation for this large Z dependence in the maximum energies includes ionization energy loss but also includes the effect described as truncation (see below).

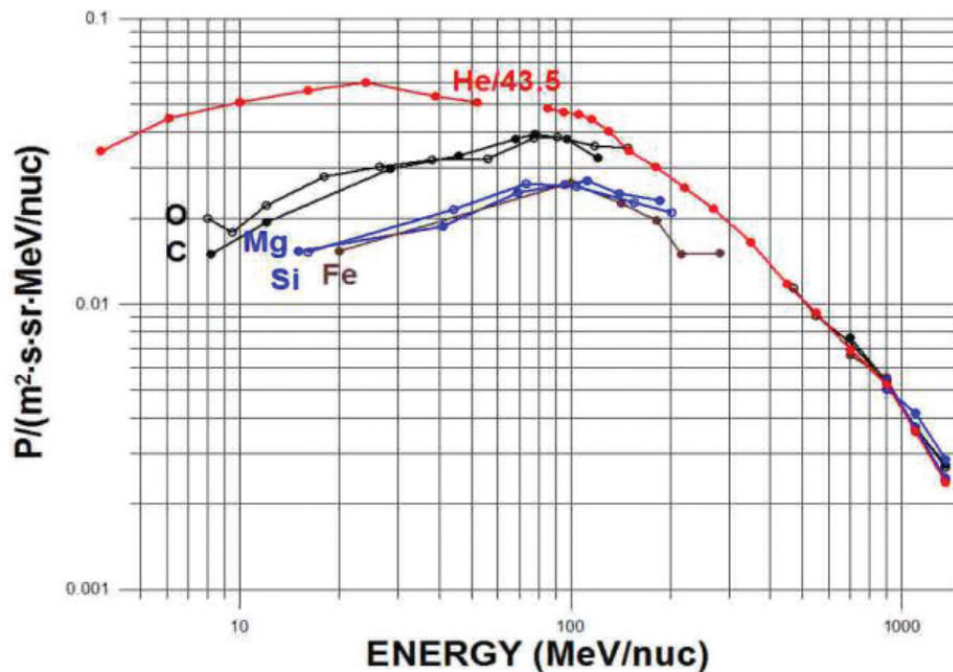


Figure 10. Observed relative intensities of He, C, O, Mg, Si and Fe nuclei between 100 and 1000 MeV/nuc. These intensities are normalized to the values of j at 1000 MeV/nuc for carbon nuclei. The figure includes lower energy intensities from [3].

In a perfect LBM for propagation in the galaxy where the sources are uniform and the propagation is effectively isotropic, the distribution of matter path length is an exponential at all path lengths with a mean path length which is \sim to the amount of matter traversed, e.g., in g/cm^2 . At low energies where this ionization loss is large enough so that the particles cannot reach us from the nearest sources, the path length distribution becomes non-exponential or truncated at small path lengths. We believe that the different shapes of these spectra at the lowest energies are the best signature of this effect. A real example of this and other low energy propagation effects have been hidden from us previously by the solar modulation effects. The impenetrable fog of almost isotropic propagation on the study of the origin and acceleration of these particles and their role in the Universe in general may, in some small way, have been lifted by these new Voyager observations.

6. Secondary cosmic rays and the mean path length in g/cm^2 in the galaxy

Isotopes such as ^2H and ^3He and charges such as Li, Be, B and so called Fe secondaries, $Z = 21-23$, are believed to have zero abundance in any possible cosmic ray source. They are therefore produced by interactions of primary cosmic rays such as He, C, O, Mg, Si and Fe, to name the most prominent, either by nuclear fragmentations the interstellar medium, or perhaps partly in or near the acceleration region itself. The presence of the radioactive decay secondary isotope ^{10}Be with a half-life of only 1.5×10^6 years as compared with the average cosmic ray life-time of 1.5×10^7 years as determined from the observed ^{10}Be abundance using

LBM diffusion [19, 20], suggests the correct scenario is one in which most of these secondary particles are produced during the extended time of a galactic diffusion process.

The isotopes ^2H and ^3He and the charge B are the most abundant and well measured of the secondary nuclei. Their cross sections for production when the primary cosmic ray nuclei interact with atoms of H and He that are part of the interstellar medium are also quite well known after years of systematic measurement.

With this as a background we show in **Figure 11** the Voyager measurements of the intensities and spectra of these three secondary nuclei. The calculated abundance for each nuclei is based on a LBM where the mean path length, $\lambda = 20.6 \beta P^{-0.45}$ above $P = 1.0$ GV and a constant path length = 9.0 g/cm^2 below 1.0 GV, and with a truncation parameter = 0.04 .

These measurements make a convincing argument that the primary cosmic rays have gone through $\sim 9 \text{ g/cm}^2$ of interstellar matter between ~ 10 and 100 MeV/nuc (~ 0.3 to 0.9 GV). At higher energies the measured B/C ratio may be used to determine the amount of matter traversed as a function of energy or rigidity. We have the V1 determination of the B/C ratio with zero solar modulation below $\sim 1.5 \text{ GeV/nuc}$ [4] and the AMS-2 determination of the ratio above $\sim 3 \text{ GeV/nuc}$ [17]. These measurements are shown in **Figure 12** along with the LBM propagation prediction using the parameters described in the above paragraph. The agreement is within $\pm 10\%$ from the lowest to the highest energies. Since this is a simple pure diffusion model, this high level of agreement at all energies implies that energy gain (reacceleration)

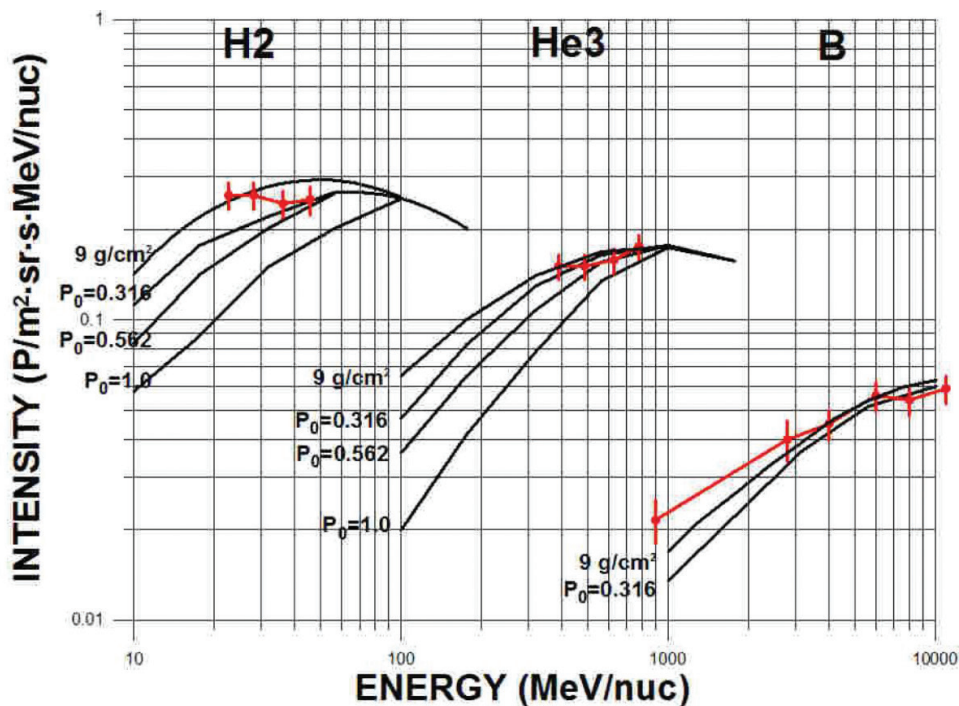


Figure 11. A comparison of the measurements of ^2H , ^3He and B nuclei intensities measured by the CRS experiment on V1 and the predictions of the LBM for values of $P_0 = 0.316, 0.562, 1.0 \text{ GV}$ and a constant path length = 9 g/cm^2 below 1.0 GV as described in the text. All three secondary isotopes are consistent with the predictions of a path length, λ , between 7 and 9 g/cm^2 at energies from ~ 20 to 100 MeV/nuc .

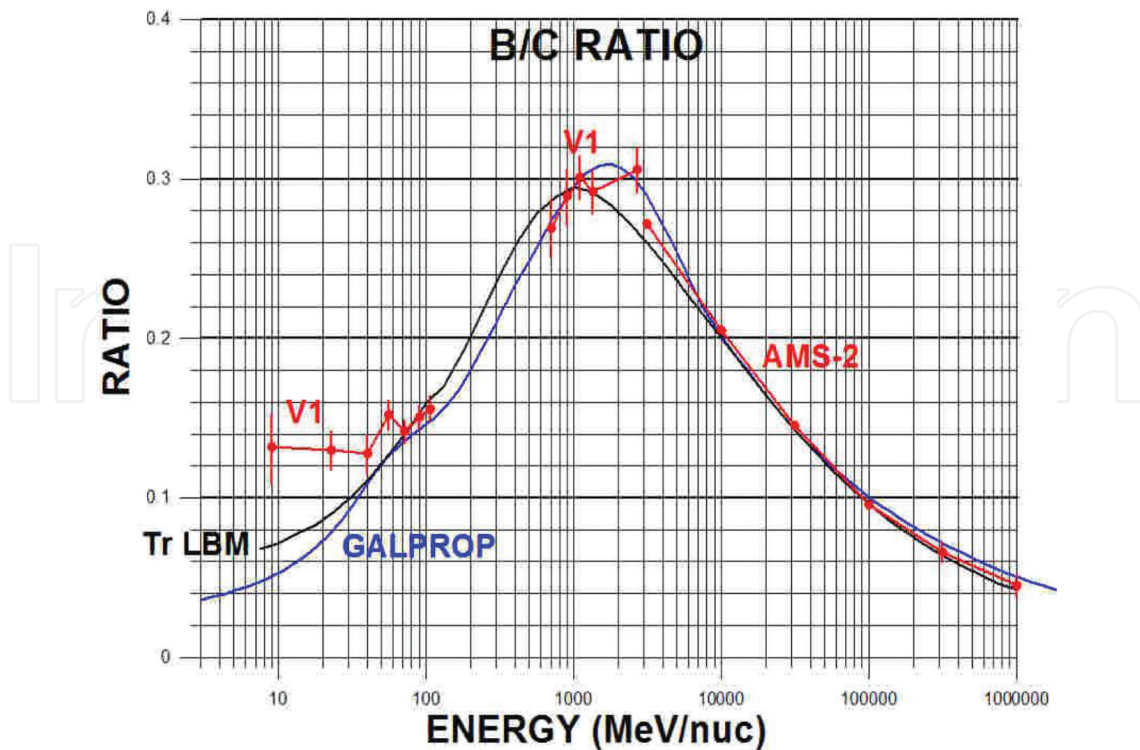


Figure 12 . The B/C ratio as a function of energy. The measurements of this ratio below ~ 2.4 GeV/nuc are from Voyager 1 beyond the heliopause [3, 4]. The higher energy measurements are from AMS-2 [17]. The calculated ratios are from the truncated LBM model described in the text and the GALPROP-DR model [3].

cannot be significant. The effects of truncation of the path length distributions at small path lengths (where the path length becomes ~ 0.6 g/cm² at the highest energies) are predicted in this model and are observed in the flattening of the B/C ratio at the highest energies [21].

7. Conclusions

So near the end of its 40 plus year mission Voyager has crossed the heliopause and sampled the interstellar energetic particle background for the 1st time. No one who has been involved in this mission from the beginning would have dreamt that this was possible. The goal of this chapter has been to attempt to convey some of the remarkable features of this data. Perhaps Voyager has saved its best for last, but only a few of us who could understand it are still around. The mission did not end with pictures of the planets but perhaps in the experience of the limits of humans in the eternal universe.

Acknowledgements

The author wishes to acknowledge his colleagues for over a generation now on the Voyager CRS team. First is Ed Stone, truly a captain of the “Starship Voyager” in the Captain Kirk tradition. Not to be outdone is Frank McDonald, our most senior advisor who sadly is no

longer with us. In fact the original “team of three” is without doubt the oldest scientifically productive team in history for a major experiment with an average age of 87.0 years. And Alan Cummings would have been part of the original team, except that he was a graduate student at the time of the 1st proposal. Now he is ready to retire, but, of course, nobody working on Voyager data would even think of that. And Nand Lal, the guru of the data system, has been around almost as long (have you ever tried the Voyager web site, <http://voyager.gsfc.nasa.gov>). There is no better one for any space experiment. And Bryant Heikkila, my former student, who can provide any data you need usually within 48-72 h real time, including the ~20 h light travel time to Earth. And last but not least, Tina Villa, who made this chapter possible.

Author details

William R. Webber

Address all correspondence to: bwebber@nmsu.edu

Department of Astronomy, New Mexico State University, Las Cruces, NM, USA

References

- [1] Webber WR. Energetic charged particles in the heliosphere from 1-120 AU measured by the Voyager spacecraft. *Astrophysics. InTech*; 2012. p. 309
- [2] Stone EC, Cummings AC, McDonald FB, et al. Voyager 1 observes low-energy galactic cosmic rays in a region depleted of heliospheric ions. *Science*. 2013;**341**:150
- [3] Cummings AC, Stone EC, Heikkila BC, et al. Galactic cosmic rays in the local interstellar medium: Voyager 1 observations and model results. *Astrophysics Journal*. 2016;**831**:19
- [4] Webber WR, Lal N, Stone EC, et al. Voyager 1 Measurements Beyond the Heliopause of Galactic Cosmic Ray Helium, Boron, Carbon, Oxygen, Magnesium, Silicon and Iron Nuclei with Energies 0.5 to >1.5 GeV/nuc. <http://arXiv.org/abs/1712.02818>; 2017
- [5] Mewaldt RA, Davis AJ, Lave KA, et al. Record-setting cosmic-ray intensities in 2009 and 2010. *Astrophysics Journal*. 2010;**723**:L1
- [6] Lave KA, Wiedenbeck ME, Binns WR, et al. Galactic cosmic-ray energy spectra and composition during the 2009-2010 solar minimum period. *Astrophysics Journal*. 2013;**770**:117
- [7] Usoskin IG, Bazilevskaya GA, Kovaltson GA. Solar modulation parameter for cosmic rays since 1936 reconstructed from ground-based neutron monitors and ionization chambers. *Journal of Geophysical Research*. 2011;**116**:A02104
- [8] Gleeson LJ, Axford WI. Solar modulation of galactic cosmic rays. *Astrophysics Journal*. 1968;**154**:1012

- [9] Beer J, McCracken K, van Steiger. Physics of earth and space environments cosmogenic radionuclides. Springer-Verlag; 2012;19
- [10] Adriani O, Barbarino GC, Bazilevskaya R, et al. Time dependence of the proton flux measured by PAMELA during the 2006 July-2009 December solar minimum. *Astrophysics Journal*. 2013;765:91
- [11] Aguilar M, Aisa D, Alvino A, et al. Precision measurement of the (e^+e^-) flux in primary cosmic rays from 0.5 GeV to 1 TeV with the alpha magnetic spectrometer on the international space station. *Physical Review Letters*. 2014;113:121102
- [12] Webber WR, Villa TL. The Galactic Cosmic Ray Electron Spectrum from 3 to 70 MeV Measured by Voyager 1 Beyond the Heliopause, What This Tells Us About the Propagation of Electrons and Nuclei In and Out of the Galaxy at Low Energies. <http://arXiv.org/abs/1703.10688>; 2017
- [13] Webber WR, Villa TL. A Comparison of the Galactic Cosmic Ray Electron and Proton Intensities From ~ 1 MeV/nuc to 1 TeV/nuc Using Voyager and Higher Energy Magnetic Spectrometer Measurements – Are There Differences in the Source Spectra of These Particles? To be submitted to arXiv
- [14] Ptuskin V, Moskalenko IV, Jones FC, et al. Dissipation of magnetohydrodynamic waves on energetic particles: Impact on interstellar turbulence and cosmic-ray transport. *Astrophysics Journal*. 2006;642:902
- [15] Aguilar M, Aisa D, Alvino A, et al. Precision measurement of the proton flux in primary cosmic rays from rigidity 1 GV to 1.8 TV with the alpha magnetic spectrometer on the international space station. *Physical Review Letters*. 2015;114:171103
- [16] Aguilar M, Aisa D, Alvino A, et al. Precision measurement of the helium flux in primary cosmic rays of rigidities 1.9 GV to 3 TV with the alpha magnetic spectrometer on the international space station. *Physical Review Letters*. 2015;115:211101
- [17] Aguilar M, Ali Cavasonza L, Ambrosi G, et al. Precision measurement of the boron to carbon flux ratio in cosmic rays from 1.9 GV to 2.6 TV with the alpha magnetic spectrometer on the international space station. *Physical Review Letters*. 2016;117:231102
- [18] Webber WR. The Different Shapes of the LIS Energy Spectra of Cosmic Ray He and C Nuclei Below ~ 1 GeV/nuc and The Cosmic Ray He/C Nuclei Ratio vs. Energy-V1 Measurements and LBM Propagation Predictions. 2017. <http://arXiv.org/abs/1711311584>
- [19] Garcia-Munoz M, Simpson JA, Guzik TG, et al. Cosmic-ray propagation in the Galaxy and in the heliosphere-The path-length distribution at low energy. *Astrophysics Journal*. 1987;64:269
- [20] Yanasuk NE, Wiedenbeck ME, Mewaldt RA, et al. Measurement of the Secondary Radionuclides ^{10}Be , ^{26}Al , ^{36}Cl , ^{54}Mn , and ^{14}C and Implications for the Galactic Cosmic-Ray Age. *Astrophysics Journal*. 2001;563:768
- [21] Webber WR, Villa TL. The Cosmic Ray Boron/Carbon Ratio Measured at Voyager and at AMS-2 from 10 MeV/nuc up to ~ 1 TeV/nuc and a Comparison With Propagation Calculations. <http://arXiv.org/abs/1711.08015>;2017